JOURNAL OF MATERIALS SCIENCE 26 (1991) 4499–4510

Analysis of isothermal and isochronal annealing in deformed Zn and Zn–Ag

B. MARCZEWSKA-LASA*, M. ZEHETBAUER, W. PFEILER, B. WIELKE
Institut für Festkörperphysik der Universität Wien, Strudlhofgasse 4, A-1090 Wien, Austria

Zn and Zn–Ag polycrystals have been deformed by rolling at 293 K to true strains $\varepsilon = 0.05$–3.8. After deformation, samples were subjected to isothermal and isochronal anneals, and thereby investigated by intermittent measurements of strength, electrical resistivity, and TEM. Along the isotherms at 293 K, quite unusual hardening effects were observed, which turned out to be strongly affected by the applied prestrain and alloy content. The experimental results can be consistently ascribed to loop formation and loop coarsening from deformation-induced vacancies whereas other explanations, such as loop formation by oxidation and/or phase transformations, can be largely ruled out. Saada's model accounts satisfactorily for the vacancy concentrations measured. In the framework of a loop-hardening theory by Kirchner, the experimentally found values of vacancy concentration and loop density/size yield the right order of magnitude for the strength effects observed. With the isochronal anneals, three stages could be found which are related to loop annealing, dislocation rearrangement, and dislocation annealing.

1. Introduction

Hexagonal metals exhibit large differences in shear stresses of different slip systems, which particularly show up in materials with large c/a ratios such as Zn and Cd. In contrast to the usual deformation of fcc metals, this leads to a marked basal slip behaviour, which has often been suggested to prevail even in each deformation stage A, B, C; this was motivated by both theoretical considerations [1, 2] as well as experimental [3–7] findings of a quite low activity in other slip systems compared with that of the basal one.

In view of these facts, it is rather surprising that the strengthening coefficient of range B still exceeds that of range A by a factor 6 [1]. Furthermore, measurements in Zn and Cd of the temperature dependence of both basal shear stress, τ_A [8, 9] and strengthening coefficient, θ [10] showed strong anomalies at about 30 K for τ_A, and 150 K for θ. Thus, a growing number of workers stressed the possibility of some interaction of deformation-induced point defects with the moving dislocations [1, 11]. For increasing strain, the point defect concentration is thought to reach such high values that even the formation of sessile loops is enabled which may resist mobile basal dislocations by Orowan-like mechanisms in stage A. Stage B is assumed to arise from the increasing long-range stress fields of these loops when exceeding a critical size, and stage C reflects the enhanced consumption of freshly created point defects by dislocations surpassing a critical density.

While approaching this thesis of a loop-hardening mechanism, the following objections to it must be discussed.

(i) Vacancy-creating jog movement after cutting events of primary dislocations with only a few forest dislocations could only provide point defect concentrations/loop densities which are far too low to satisfy the magnitude of the strength effects observed.

(ii) There exists another mechanism of (vacancy) loop formation, preferably arising in oxide-layered Zn and Cd crystals, especially in cases of specimens with a large surface being usually prepared for TEM investigations [12–16].

It was the aim of the present work to check on prior results by Mikulowski *et al.* [9], where extraordinary strength(ening) effects were observed during 293 K annealing immediately after deformation at 4.2–150 K; these could be related far better to deformation-induced vacancy loops and their coarsening rather than to any interaction between dislocations. Alternatively, the present work intended to study deformation and/or annealing effects with large strains instead of low temperatures. Therefore, the concentration of vacancies should be strongly enhanced, in spite of the rather high deformation temperature 293 K. Variation of plastic strain as well as application of adequate annealing treatments (isotherms and isochrones) should enable the separation of effects possibly caused by point defects from those by dislocations and grain boundaries, and further on the control of the number and size of any point defect clusters interacting with dislocations.

2. Experimental procedure

2.1. Deformation methods and strength tests

Polycrystalline rods of Zn and Zn–0.4 at %–Ag

* *Present address*: Instytut Przerobki Plastycznej i Metaloznawstwa, Akademia Gorniczo-Hutnicza, 30-059 Krakow, Poland.

0022–2461/91 $03.00 + .12

(denoted Zn0.4Ag) of purity 99.998% were annealed for 5 h at 500 K; almost no recrystallization took place (see also Section 3.2.3.). The resulting grain sizes were 15 μm (Zn) and 30 μm (Zn0.4Ag). Plastic deformation was achieved at a deformation temperature $T = 293$ K by straight rolling to final true strains $0.05 < \varepsilon < 3.8$, where small and equal rolling steps were applied, $\Delta\varepsilon = 0.1$. The final thickness of the samples was approximately kept constant over ε, $h_f \approx 0.2$ mm, in order to obtain comparable deformation states [17].

Intermittent measurements of microhardness were preferred to analogous ones of yield stress for the following reasons.

1. In contrast with yield stress measurements, microhardness tests can be performed repeatedly on one single sample without any influence on strength caused by the testing method itself; this condition is of great importance if one is interested in highly accurate strength measurements with isothermal/isochronal treatment.
2. Comparative studies between the two methods on the same samples showed identical isothermal/isochronal strength characteristics, after having corrected the values of yield stress for test-involved deformation.

The respective tests were carried out with a Reichert microhardness tester installed in a Reichert MeF inverted light microscope; 20 indentations per value were performed, at a load of 0.289 N and an indentation rate of $0.003\ \mathrm{mm\,s^{-1}}$. This way, a relative accuracy of $\pm$ 1% resulted. With the isochrones connected, samples were heated in a furnace in an Ar atmosphere and held for 10 min at each temperature. The step of each temperature increase was 10 K.

2.2. Measurements of residual electrical resistivity

These measurements generally served to attain values of deformation-induced defect densities. They were performed by a standard potentiometric method usually in liquid N_2, only one isochrone (Fig. 6c) was achieved in liquid He. The samples were cut by spark erosion. A resolution of less than 10^{-3} could be realized at a current of 1 A. For details of isochronal treatment, see Section 2.1.

2.3. Optical investigations

Optical investigations were carried out by light microscopy (LIM, Reichert MeF) as well as by transmission electron microscopy (TEM, Siemens Elmiskop 1A and Tesla 613) operated at 100 kV. For the LIM observations, samples of Zn were chemically polished in two reagents alternately:

Reagent 1: 160 g CrO_3, 20 g Na_2SO_4, 0.5 l distilled water

Reagent 2: H_2O_2 concentration 30%, HNO_3 concentration 16N, in solution with methanol.

Samples of Zn0.4Ag were polished electrolytically in a hydrous solution of CrO_3, 1:5, at about $0.03\ \mathrm{A\,mm^{-2}}$ and rinsed in methanol.

Sample preparation for TEM was achieved in two steps. First, they were thinned in a Struers double-jet equipment in a hydrous electrolyte of H_3PO_4, 1:5.8, at $0.6\ \mathrm{A\,mm^{-2}}$ and about 10 °C. Second, they were polished manually in a solution of H_3PO_4 and C_2H_5OH in equal parts, at a voltage of 2.5–3 V and 20 °C. Unfortunately, a large percentage of samples had to be discarded, because they had a strong tendency to oxidize immediately after preparation when being stored at 293 K.

For details of isochronal treatment, see Section 2.1.

3. Results

3.1. Isothermal annealing

3.1.1. Mechanical properties

Microhardness tests were performed immediately after deformation at $T = 293$ K and in intervals not exceeding 2 h up to about 1 day, while storing the samples at an annealing temperature, $T_a = 293$ K. The samples did not show any usual recovery behaviour. At small deformations, pure Zn exhibited a strength decrease of about 20% (Fig. 1a), but underwent an intermediate increase and further decrease contrary to the expected monotonic recovery. The heavily deformed Zn also exhibited some unusual annealing characteristics, namely a (although quite less marked) strength minimum (Fig. 2a). In slightly deformed Zn0.4Ag (Fig. 1b), the strength even increased to an absolute maximum, and after 24 h it adjusted roughly to the value of the strength immediately after deformation. Strongly deformed ZnAg (Fig. 2b) showed the most drastic effects: here the strength first decreased by a factor of 2.3 within a few minutes, and then again increased by a factor of 2.5 within 14 h before reaching a constant value.

3.1.2. Optical investigations

Observations were performed by light microscopy (LIM) as well as electron microscopy (TEM) preferably in ZnAg, parallel to the measurements of mechanical properties. Preparation time for TEM was kept ≤ 2 h after deformation in order to avoid annealing effects before investigation. Together with some prior findings of our group [18, 19] we resume some evidence for the existence and growth of dislocation loops. After an annealing time, $t_a = 2$ h after deformation $\varepsilon \leq 0.15$, the loops had an average diameter $d \approx 0.2$ μm and a density $N_v \approx 8$ loops/μm^3 (Fig. 3a, b), whereas for $t_a > 5$ h they grew to diameters $d \approx 0.5$ μm and densities $N_v \approx 3.5$ loops/μm^3 (Fig. 3c). These results were revealed to be rather insensitive to the sort of solved atoms, deformation temperature as well as the kind of crystals used. Although due to the oxidation problems only a very small number of samples could be evaluated (which especially led to rather uncertain values of N_v), and in spite of some undoubted loop growth effect by heating through the electron beam, it seems important to mention that

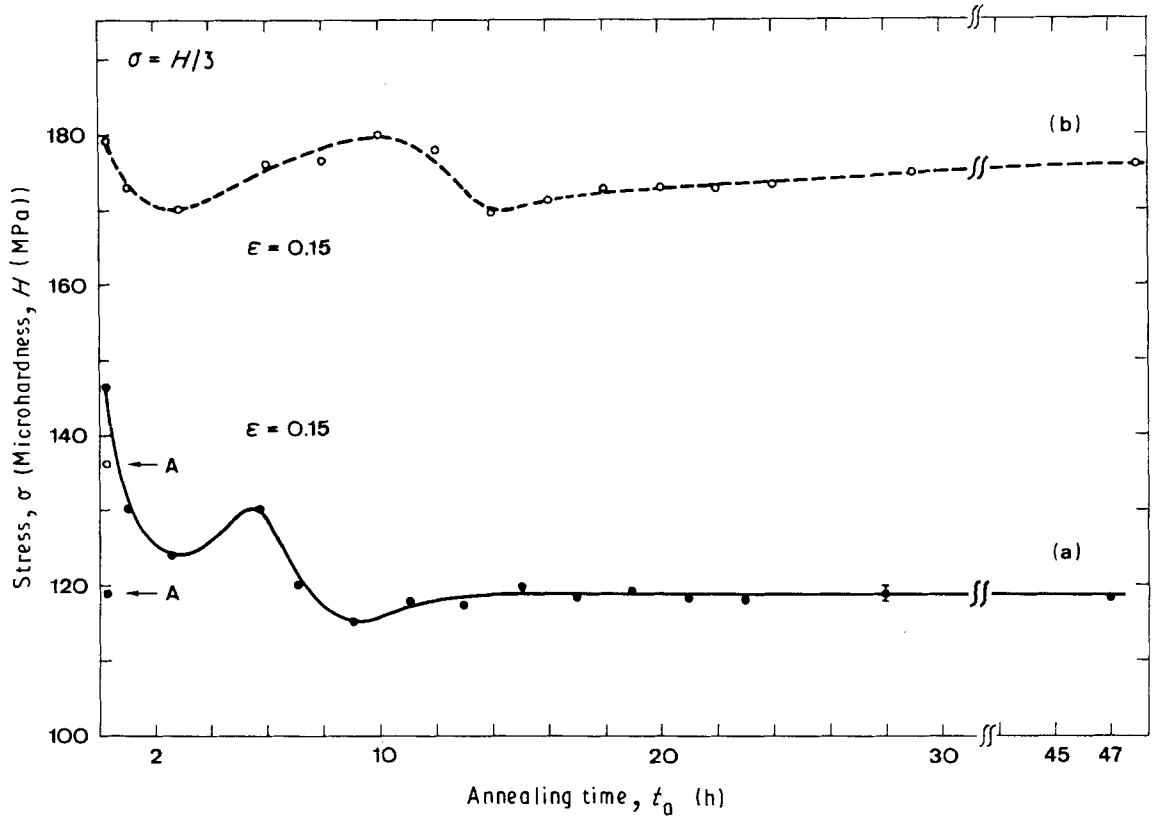

Figure 1 Stress isotherms at $T_a = 293$ K, after deformation at $T = T_a$ to low strains, ε, as indicated. A denotes the stress level of the annealed state. (a) Zn, (b) Zn0.4Ag.

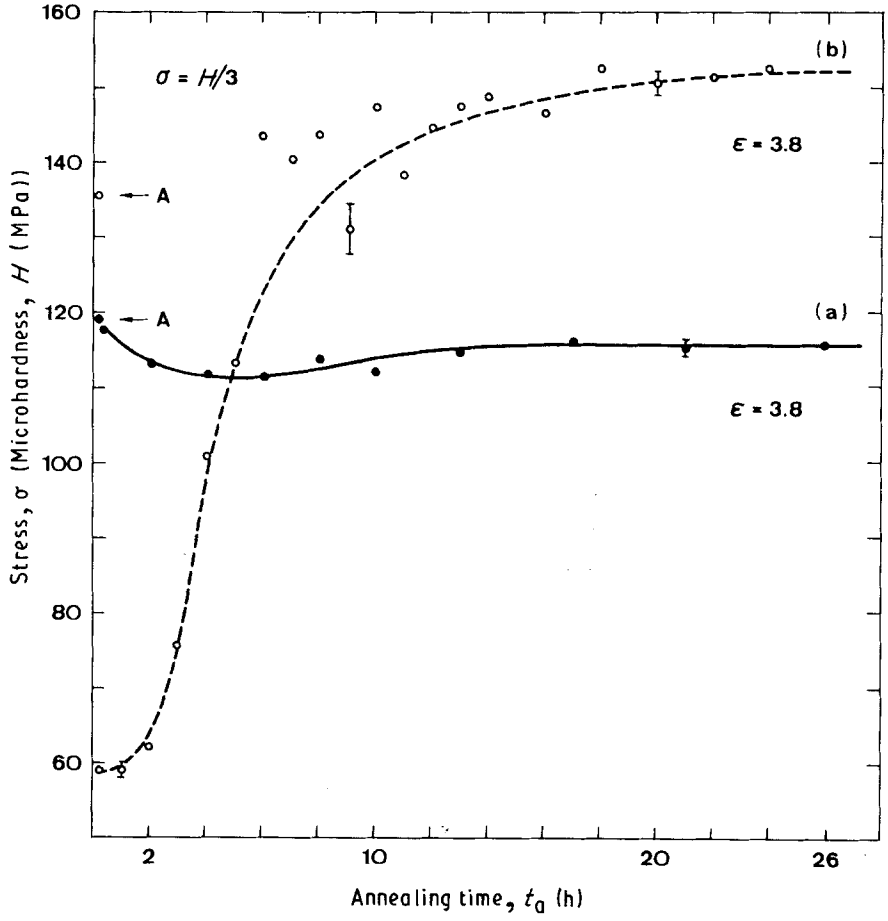

Figure 2 Stress isotherms at $T_a = 293$ K, after deformation at $T = T_a$ to high strains, ε, as indicated. A denotes the stress level of the annealed state. (a) Zn, (b) Zn0.4Ag.

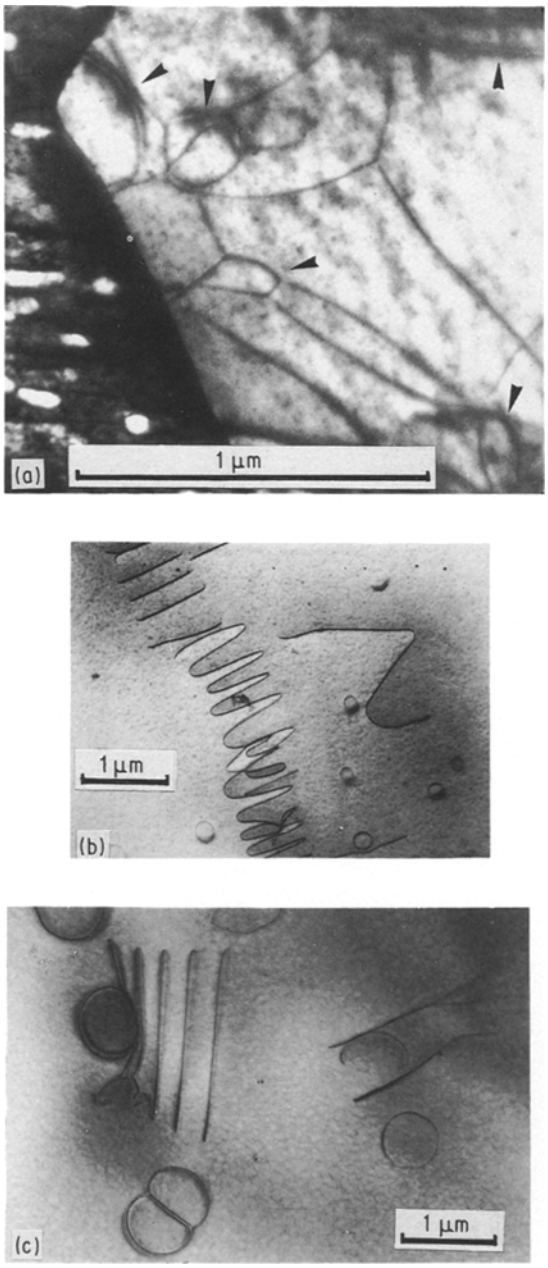

Figure 3 Loop formation and coarsening in deformed Zn alloys (polycrystals, true strain ε; single crystals, shear strain *a*). (a) Zn0.4Ag, $\varepsilon = 0.15$, $T = T_a = 293$ K, $t_a = 2$ h; arrows indicate loops; (b) Zn0.2Ga, $a = 0.05$, $T = 77$ K, $T_a = 293$ K, $t_a = 1.5$ h [19]; (c) Zn0.2Ga, $a = 0.04$, $T = 77$ K, $T_a = 293$ K, $t_a > 5$ h [18].

both loop sizes and loop densities match well several previous findings in the literature for pure Zn [20–22]. The average size of cells as well as that of grains did not change within the observation time.

3.2. Isochronal annealing

3.2.1. Mechanical properties

The mechanical properties were studied partially by yield stress tests, but mainly by microhardness tests for the reasons given in Section 2. Isochronal annealing characteristics were followed by temperature steps of 10 K with samples that had been deformed to various strains, for both Zn and Zn0.4Ag. In principle, three annealing stages were found, of which Stages II and III shifted to lower temperatures with increasing applied strain (Table I, and Fig. 4a, b for low strains, Fig. 5a, b for large strains). In pure Zn, however, neither a Stage II, nor a distinct shift to lower temperatures of any stage could be observed.

3.2.2. Resistivity measurements

In pure Zn, the most distinct annealing step was observed at temperatures close to that of Stage III using the terminology of microhardness results (Fig. 6a). However, in Zn0.4Ag, some Stage I/State II annealing behaviour was also found (Fig. 6b), although this is not so well developed as in the case of the microhardness isochrones. Again a shift of Stages II and III to lower temperatures with increasing strain could be clearly identified for Zn0.4Ag, but not for pure Zn (see Table I). To obtain more information on Stage I, a single isochrone in Zn was performed in the following way. The sample was stored at $-196\,^{\circ}C$ immediately after rolling at $T = 293$ K, and then measured isochronically between $T_a = -180\,^{\circ}C$ and $T_a = 140\,^{\circ}C$ (Fig. 6c). Here, a rather high and wide Stage I resulted, and also Stage III could be observed (see Table I).

3.2.3. Optical investigations

Similar to isothermal treatment, observation by light microscopy (LIM) as well as electron microscopy (TEM) was performed parallel to microhardness isochrones. The LIM investigation revealed the grain size, d_g, of both materials, Zn and Zn0.4Ag, to be roughly constant up to temperatures $T_a = 170\,^{\circ}C$ ($d_g = 17$ μm for Zn, $d_g = 30$ μm for ZnAg), and then showing a slight tendency to grow (by a factor 1.5) close to temperatures $T_a = 200\,^{\circ}C$. Using TEM (Zn0.4Ag, $\varepsilon = 0.15$), a cell structure of dislocations was observed; the average cell size, d_c, was found to stay constant ($d_c = 2$ μm) up to about $T_a = 130\,^{\circ}C$ (Fig. 7) which coincides with the occurrence of Stage II at corresponding values of applied strain. Beyond that temperature, the cells converted into subgrains (sharp contrast of cell wall arising from single dislocations), their size now reaching $d_s = 8$ μm on average (Fig. 8). The subgrains frequently exhibited groups of single dislocations in their interior. At approximately $T_a = 170\,^{\circ}C$ (indicating Stage III), a uniform structure of coarsened subgrains was observed, together with a few groups of single dislocations in their interior once more. The typical subgrain size now amounted to $d_s = 15$ μm being already close to the grain size revealed by LIM at this annealing temperature (for comparison with the above measurements, see Table I).

4. Discussion

4.1. Isothermal annealing

The variations in strength observed on annealing at 293 K deviate strongly from usual recovery effects, e.g. in fcc metals [23], with respect to both the amount of annealing and its characteristics. According to the discussion of analogous features in previous papers of our group [9, 18, 19], it seems worthwhile to consider

TABLE I Temperature positions, $T_a(i)$ of annealing stage (i), in Zn and Zn0.4Ag, as a function of applied strain, ε, for the various methods quoted for isochronal investigation (deformation temperature $T = 293$ K)

Method	Material	ε	T_a(I) (°C)	T_a(II) (°C)	T_a(III) (°C)
Microhardness	Zn	0.05	20–60	–	110–230
(yield stress)	Zn	3.8	20–50	–	110–160
	Zn0.4Ag	0.15	20–50	120–130	170–200
	Zn0.4Ag	3.8	20–50	80–100	140–160
Resistivity	Zn[a]	0.15	(– 180)–20	–	50–140
	Zn	0.5	–	–	100–170
	Zn	3.8	–	–	100–190
	Zn0.4Ag	0.05	20–50	90–170	170–250
	Zn0.4Ag	0.15	20–50	50–170	170–230
	Zn0.4Ag	0.5	20–50	70–100	100–220
TEM	Zn0.4Ag	0.15	70	130	170
cell, subgrain			cells	cells and subgrains	subgrain coarsening
size (μm)			2	8	15
misorientation (deg)			2	6	6

[a] Sample stored at 77 K after deformation; evaluation from resistivity isochrone in Fig. 6c.

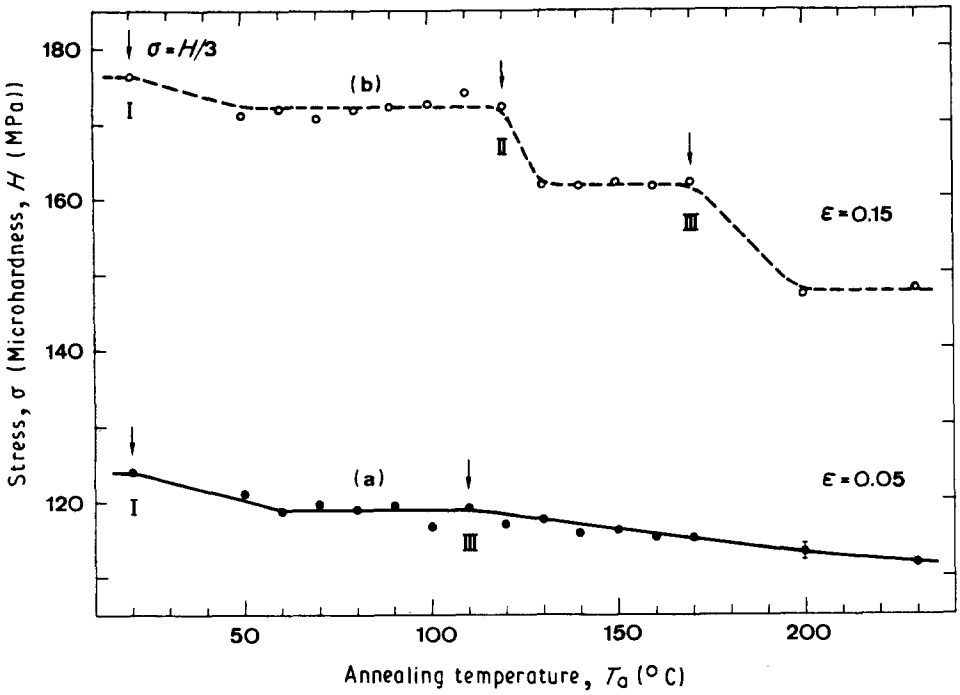

Figure 4 Stress isochrones for $T_a > 293$ K, after deformation at $T = 293$ K to low strains, ε, as indicated. The arrows denote the onset of the annealing stages. (a) Zn, (b) Zn0.4Ag.

the deformation-induced generation of point defects (namely vacancies) and their accumulation to defect clusters, which could affect the strength behaviour as observed. The occurrence of vacancies is strongly confirmed by the resistivity characteristics shown in Fig. 6c (for further details see next section): Here, intensive defect annealing is indicated at temperatures $T_a > 110$ K where various experiments in irradiated Zn [24–26] and deformed Zn [27, 28] report the onset of vacancy migration. Moreover, this peak has been equally found by calorimetric measurements [29] which revealed an activation enthalpy $Q = 0.30$ eV very close to the migration enthalpy of vacancies in Zn [30]. Fig. 6c also exhibits some evidence for vacancy clustering: the annealing temperatures of the first step span quite a large range of temperatures (reaching ~ 293 K) which is typical of the combined annealing of single vacancies and vacancy clusters (loops*) of various sizes. In contrast to single vacancies [31], vacancy loops act as certain barriers to dislocation movement and thus can cause drastic effects to macroscopic strength, as is well known from isothermal behaviour of metals after rapid quenching [32] (see also next paragraph). Kirchner [11] formulated a theory based on an Orowan-like mechanism which calculates the strength increase, $\Delta\tau$, from vacancy

* From TEM observations [20, 21] as well as from positron-annihilation studies [27, 28], the formation of three-dimensional vacancy clusters can be ruled out.

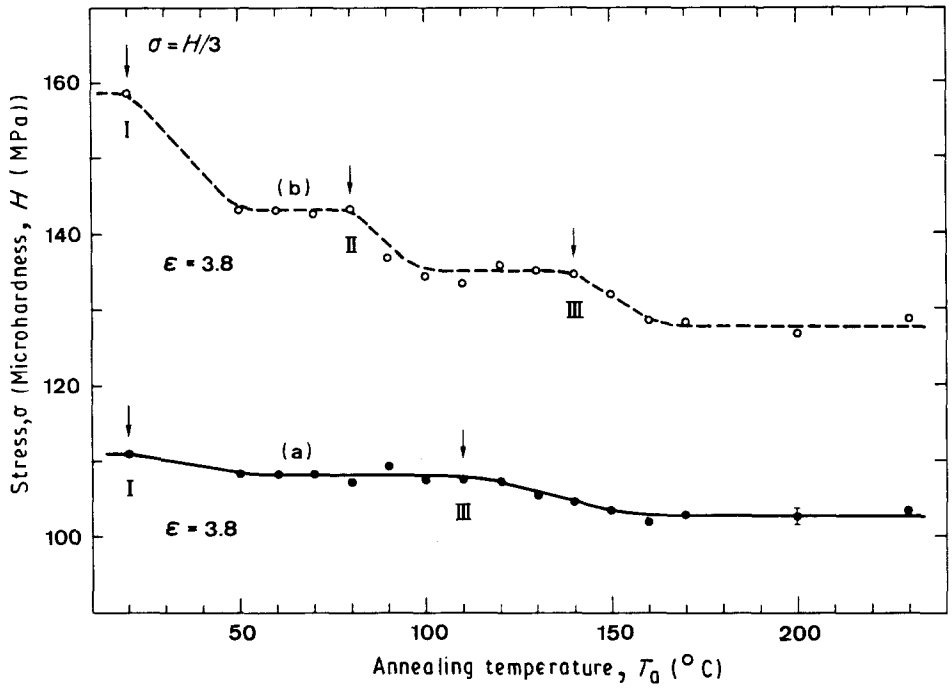

Figure 5 Stress isochrones for $T_a > 293$ K, after deformation at $T = 293$ K to high strains, ε, as indicated. The arrows denote the onset of the annealing stages. (a) Zn, (b) Zn0.4Ag.

loops also during loop coarsening, as demonstrated in Fig. 9. The analogies to Figs 1 and 2 are quite evident, thus giving motivation for a rough check of the theory's main relations by the actual experimental values. For example, the theory predicts a minimum in $\Delta\tau$ to occur when

$$N_v^{-1/3} d^{-1} \approx 6 \qquad (1)$$

where d is the average loop diameter, and N_v is the number of loops per unit volume. From the step height of the resistivity in Fig. 6c, a vacancy concentration $c_v = 4.1 \times 10^{-5}$ results; Transmission electron micrographs from samples deformed $\varepsilon = 0.15$ at $T = 293$ K and annealed for $t_a = 2$ h (which corresponds to the minimum (Equation 1) in strength) yielded values of $d \approx 0.2$ μm, $N_v \approx 8$ loops/μm^3; because these values give $c_v = 5 \times 10^{-5}$ in good accordance with the above resistivity result, they may be inserted into Equation 1: a value of 2.3 for the product results. This is in good agreement with the theory, in view of the difficulties in TEM preparation quoted in Section 2, which especially lead to rather uncertain values of loop density, N_v.

Kirchner's theory also provides a check of the strength increase by Equation 8 of his paper [11]. Taking the correct values for k and a in this equation with respect to the certain value of $N_v^{-1/3} d^{-1}$, and using the experimental results for c_v, N_v from above, and $d = 0.2$–0.5 μm, the loop-induced strength increase can be calculated to be about a factor of 5; this is also in good agreement with the actual experiments which give a result of up to a factor of 2.5, bearing in mind that in the experiment the volume fraction of vacancies/vacancy loops would certainly not stay constant because of some annealing at 293 K.

Comparison with other experimental features confirms this picture of the supersaturated vacancies playing a dominant role in strengthening processes in Zn (and in hcp metals generally).

(i) Strength investigations by Fegredo [33] which were made immediately after quenching Zn from near the melting point, revealed the vacancy-induced hardening effect to reach almost a factor of 10; additional hardening by a factor of 1.2 occurred during isothermal annealing at 293 K, followed by an equal-sized decrease down to about the quenched-in strength; based on the above discussion, conclusions of analogy to coarsening of loops are justified.

(ii) The recovery effect during relaxation of Zn at 293 K is of the order of $\Delta\tau \cong -20\%$ ([1, 2], and present work), which markedly exceeds the value of -10% usually observed for fcc metals at comparable temperatures $T = 0.4\ T_m$ [23] (T_m is the melting temperature, K): this difference is suggested to be due to the different effect deformation-induced vacancies have on the dislocation rearrangement in hcp metals, where it is enhanced by both the favoured site of vacancies (loops) in basal planes as well as favoured slip of dislocations therein, compared to fcc metals.

In the ZnAg isotherms investigated, the related effects become even more drastic; thus, any recovery will be covered (low ε) or even greatly overcompensated (high ε) so that the stress will increase strongly and finally remain constant (strength increase of a factor of 2.5 for high ε, Fig. 2b). A similarly large effect (factor of 2.5 in strength) has already been observed by Mikulowski *et al.* [9] after annealing single-crystal Zn0.2Ag at $T_a = 293$ K, which had previously been weakly deformed at $T = 77$ K. We conclude that the clusters formed from originally single vacancies would be distinctly more stable in the alloy than in pure Zn, at least at an annealing temperature $T_a = 293$ K. These facts are once more confirmed by the experiments of Fegredo [33] who found the strength caused by

quenched-in vacancies and clusters to be stable against storage at 293 K.

4.2. Isochronal annealing

4.2.1. Stage I

Stage I is developed markedly in samples of ZnAg, and slightly in those of Zn, and appears more distinctly in the isochrones of microhardness than in those of resistivity (Figs 4–6, except for the 77 K isochrone). Electrical resistivity measurements in deformed crystals mainly reflect the number of crystal defects (actually, vacancies, and dislocations for densities $N > 10^9\,cm^{-2}$), regardless of their specific dilatation fields [34]. This, in principle, enables the determination of deformation-induced vacancy concentration and/or dislocation density as a function of strain, ε, for both materials, the results of which are presented in Table II.

As a consequence of the discussion in Section 4.1, we are led to the opinion that Stage I is represented by the annealing of deformation-induced surplus vacancies/vacancy loops. This view is corroborated by two further facts.

(i) Via the concentration of the deformation-induced vacancies, the size and, thus, the stability of the loops could be enhanced at extended strains, ε, particularly in the case of coexisting impurities. This explains why the step height in the 293 K isochrones increases with increasing applied strain; this fact, however, is more evident from microhardness (Figs 4, 5) than from resistivity (Fig. 6). On the other hand, the sensitivity of microhardness to the size of loops is much larger than that of resistivity, so that the above picture of a largely coarsened vacancy loop structure is confirmed.

(ii) Stage I does not shift to lower temperatures for increasing applied strain; thus the annealing kinetics of the defects in question cannot be greatly assisted by local stress, which agrees with the fact that the stress field of vacancies/vacancy clusters falls with $1/r^2$, instead of $1/r$ (r is the distance from the defect) of, for example, dislocations, as discussed in Section 4.2.3.

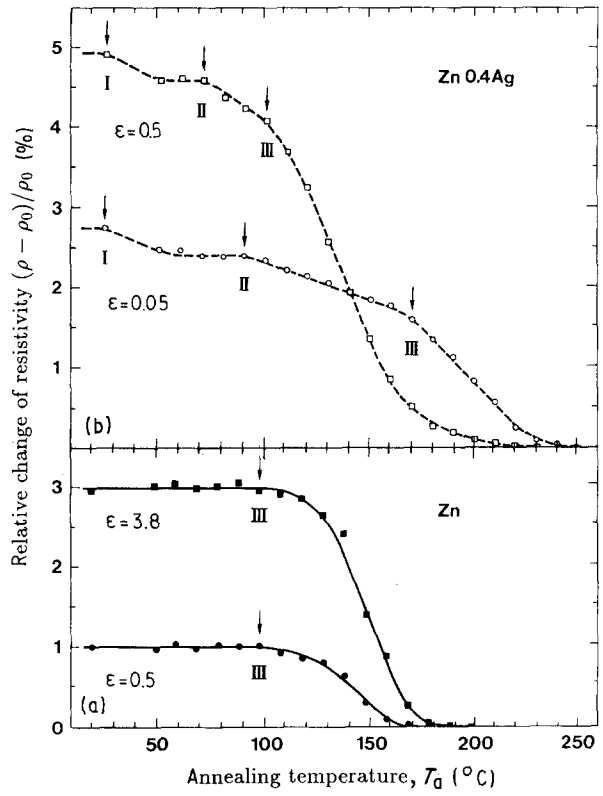

Figure 6 Resistivity isochrones, after deformation at $T = 293$ K to low and high strains, ε, as indicated. The arrows denote the onset of the annealing stages. ρ_0 is the resistivity of totally annealed state, $\rho_0 = 1.16\ \mu\Omega$ cm. (a) Zn, $T_a > 293$ K, (b) Zn0.4Ag, $T_a > 293$ K, (c) Zn, $T_a > 77$ K.

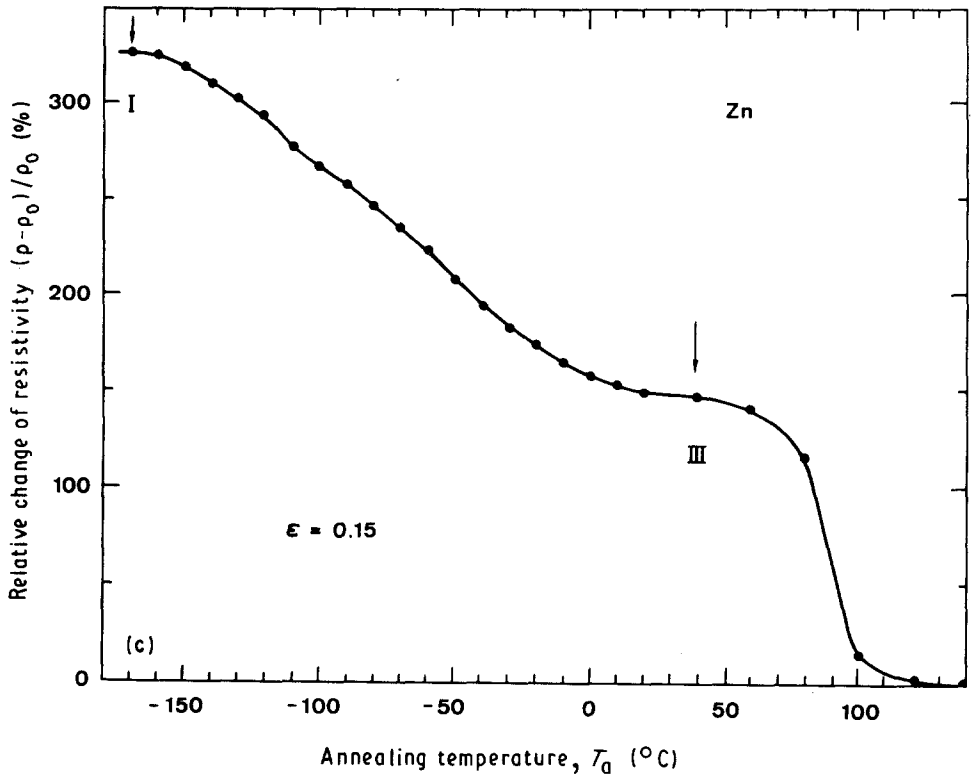

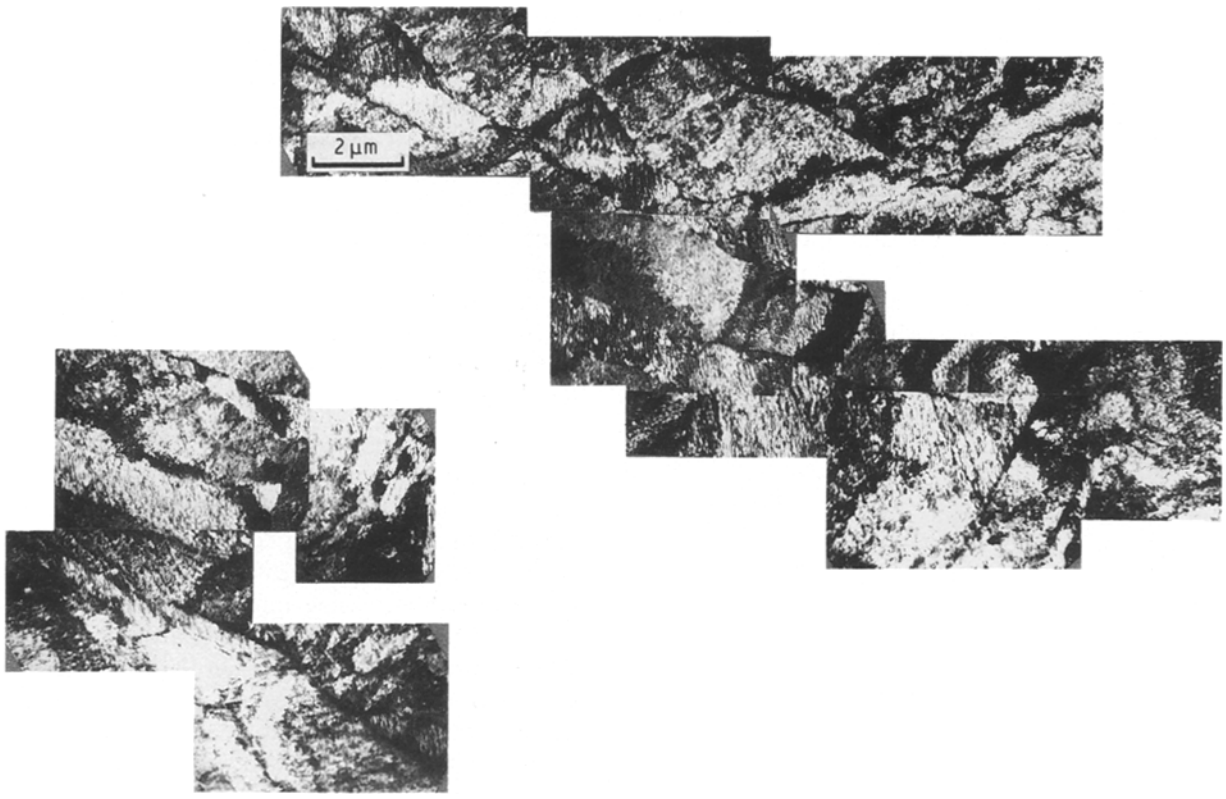

Figure 7 Transmission electron micrographs of dislocation cells after isochronal annealing up to $T_a = 70\,°C$ (Zn0.4Ag, $\varepsilon = 0.15$).

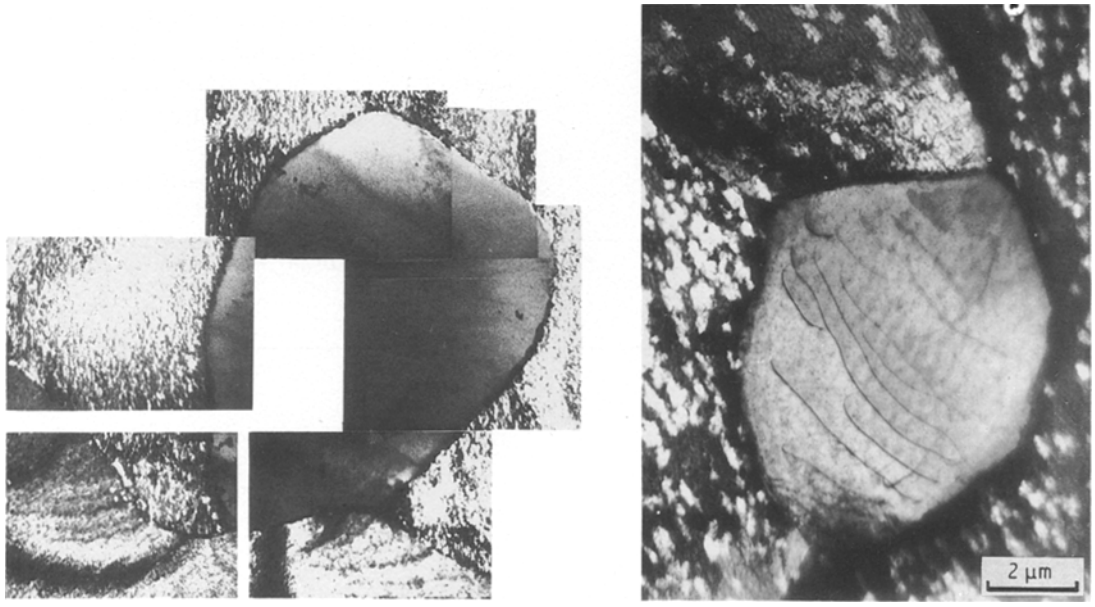

Figure 8 Transmission electron micrographs of dislocation subgrains after isochronal anneal up to $T_a = 130\,°C$ (Zn0.4Ag, $\varepsilon = 0.15$). On the right, note the considerable number of extra dislocations in the subgrain interior.

This fact has been equally observed in a calorimetric study of low-temperature deformed Zn single crystals [29].

4.2.2. Stage II

Stage II was also mainly observed in ZnAg (Figs 4b, 5b, 6b), at temperatures that became lower, with increasing applied strain. Values of resistivity at the temperatures in question, mainly reflect the evolution of dislocation density after annealing of deformation-induced vacancies; because the resistivity neither decreases strongly nor changes its rate of decrease significantly, we conclude that structural reorganizations of dislocations will take place without a marked loss in average dislocation density. This picture is confirmed by the TEM investigations which demonstrate the onset of subgrain formation at this stage (Fig. 8) from the original cell structure (Fig. 7). In our opinion, the fact that in pure Zn this stage has not been observed, even at the microhardness isochrones, again hints at some effect of friction stress in the Zn

TABLE II Densities of deformation-induced lattice defects (c_v = vacancy concentration, N = dislocation density), evaluated from measurements by electrical resistivity and by TEM (deformation temperature $T = 293$ K)

Method	Material	ε	c_v ($\times 10^{-5}$)	N (10^{10} cm^{-2})
Resistivity	Zn[a]	0.15	4.1	1.57
	Zn	0.15	0	0.32
	Zn	0.5	0	1.61
	Zn	2.0	0	4.03
	Zn	3.8	0	4.83
	Zn0.4Ag	0.05	1.2–1.3	2.2–3.9
		0.15		
	Zn0.4Ag	0.5	1.3	7.38
	Zn0.4Ag	2.0	?	7.83
TEM	Zn0.4Ag	0.15	5	1.17

[a] Sample stored at 77 K after deformation; evaluation from resistivity isochrone in Fig. 6c.

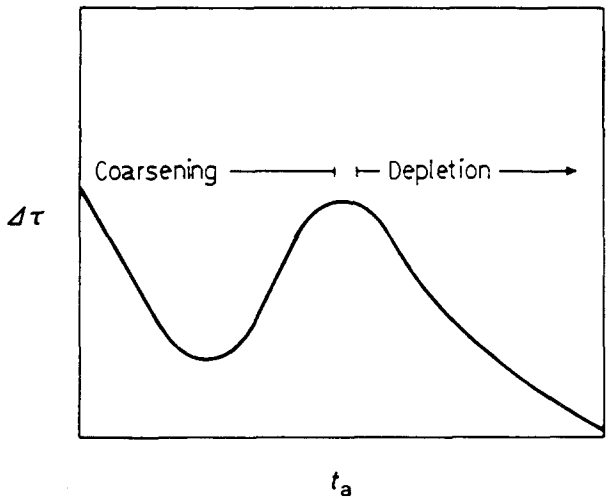

Figure 9 Sketch of loop hardening, Δτ, as a function of annealing time, t_a (from [11]). The relative minimum is reached for a loop size/distribution as given by Equation 1 (see text).

alloy: it implies an enhanced stability of deformation-induced dislocation structures resulting in a more selective annealing response compared with pure Zn.

4.2.3. Stage III

The drastic decrease in both strength (Figs 4, 5) and electrical resistivity (Fig. 6) should be ascribed to a significant loss in dislocation density. First, this would be in accordance with recent findings by positron annihilation [27, 28] and calorimetry [29]; secondly, our experimental results from TEM (Figs 7, 8) confirm this interpretation. For the case of Zn0.4Ag and $\varepsilon = 0.15$, we could ascertain a subgrain-dominated structure and its coarsening by TEM (Table I), and found a factor of 2 in subgrain size increase between annealing temperatures $T_a = 130$–$170\,^{\circ}$C. By using the well-known Burgers relation giving the dislocation density, N, from misorientation, θ, between adjacent subgrains of size d_s, and by using the respective values in Table I, one gains $N \approx 1.17 \times 10^{10}$ cm^{-2} as the difference of dislocation densities before Stage II and beyond Stage III. This value for N lies below that calculated from resistivity measurement ($N \approx 3.9 \times 10^{10}$ cm^{-2}, Table II), although the heights of Stages II and III have again been taken as a measure of N. The remaining difference may be explained by the fact that, in some grains, comparably high densities of individual dislocations were observed (Fig. 8). In our opinion, these could emerge during the cell's transformation to subgrains, reflecting the fact that not all cell dislocations can be used to form new subgrains, especially in cases of strongly anisotropic slip, as in the Zn and ZnAg materials investigated here.

Similar to Stage II, a deformation-induced shift of Stage III to lower temperatures occurred. As mentioned, this is a well-known effect in dislocation annealing which results from internal stresses of the dislocations themselves, their level being expected to increase with growing deformation strain [17, 35, 36]. Again, in ZnAg the lattice defects (dislocations here) appear to be somewhat pinned compared with pure Zn, leading to ~ 30–60 K higher temperatures of the Stage III annealing.

4.3. The dependence of annealing effects on applied strain

Strain-dependent effects can be roughly subdivided into vacancy- and dislocation-dominated ones. These have been exhaustively treated in the last two sections and can be separated by means of selective step analysis with isochronal annealing. The stress–strain characteristics of both Zn and ZnAg in principle undergoes a sharp maximum at about the same strain value (Fig. 10) and then falls off drastically, even reaching strength values mostly lying below* those of the undeformed state. This effect has already been found by Deighton and Parkins [37], which they interpreted in terms of dynamic recovery. The present experiments yield additional information from electrical resistivity measurements giving the strain dependence of dislocation density, N (Fig. 11): with respect to ε, N increases monotonically so that one cannot interpret the maximum stress, σ, by means of a similar maximum of N. Although being more marked, the nature of softening appears to be quite similar to that found previously in Al and Cu [17]. Thus, the present softening is also suggested to be a consequence of stress-aided energy-lowering rearrangements of dislocations without substantial losses in N, typically being rather a static than dynamic process. This may be additionally confirmed in the actual case by the strain shift of the maximum strength and by the lowering of its extent during isothermal annealing at $T_a = 293$ K, particularly in pure Zn (Fig. 10a). Nevertheless, these rearrangements need dislocation climb in order to operate and thus can be realized only by assistance of coexisting surplus

* Except for loop-formation effects (Fig. 10b, arrow), which have already been discussed in Section 4.2.

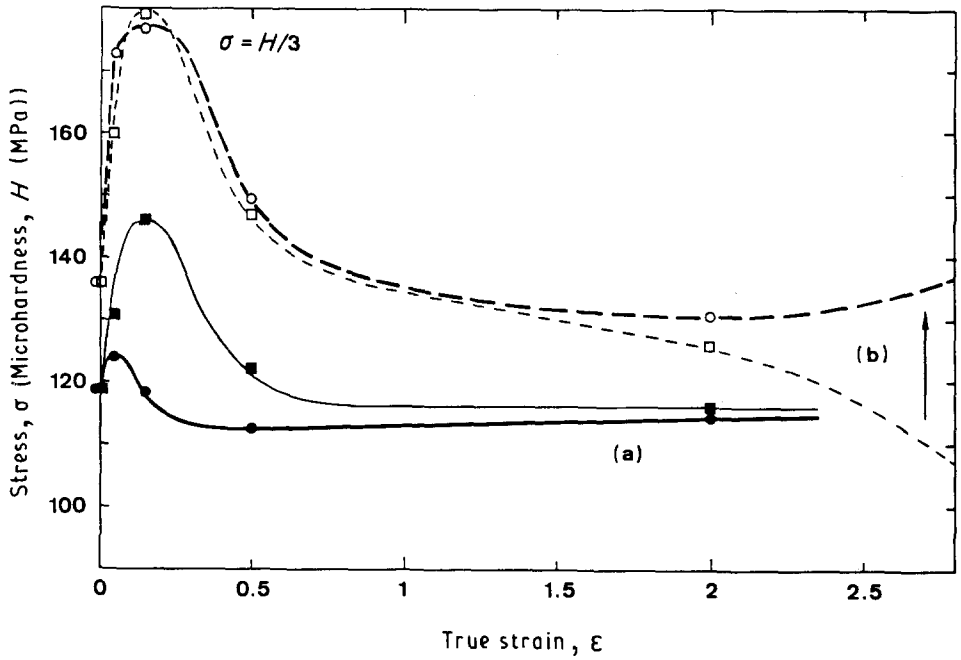

Figure 10 Stress, σ, as a function of deformation, ε ($T = T_a = 293$ K) for annealing times, t_a, as indicated. (a) Zn, (b) Zn0.4Ag. Note the effect of anneal hardening (arrow) in (b). t_a: (□, ■) 15 min, (○, ●) 24 h.

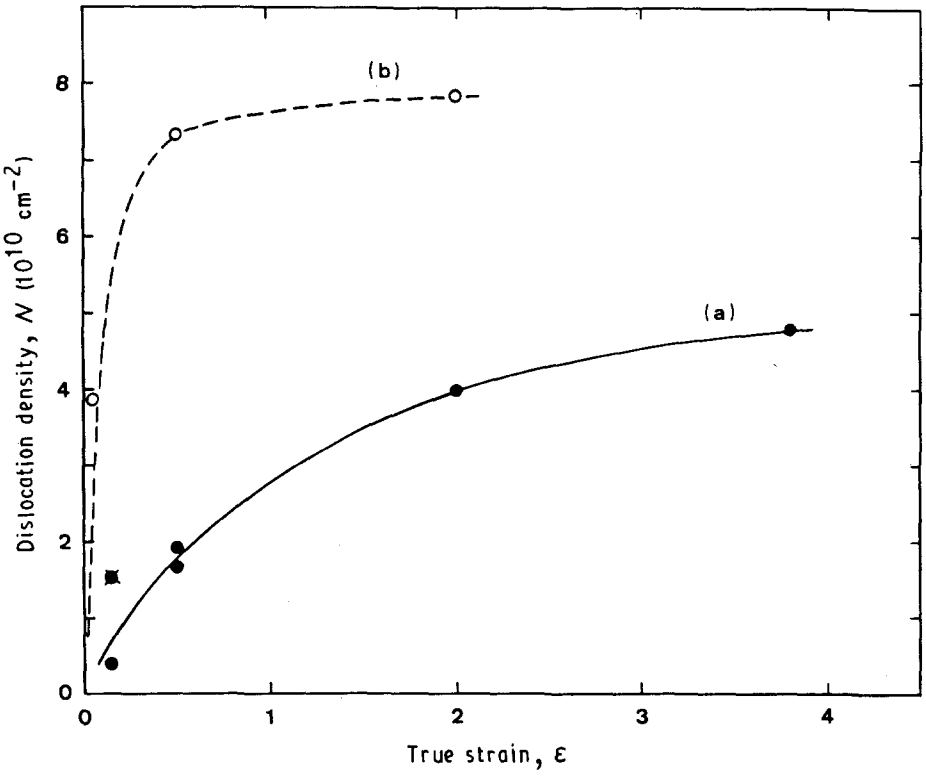

Figure 11 Dislocation density, N, derived from resistivity isochrones given in Fig. 6, having taken the sum of Stages II (if any) and III (exact values see Table II). (a) Zn: (●) Fig. 6a, (■) Fig. 6c; (b) Zn0.4Ag.

vacancies [17], with some critical minimum concentration to launch the climbing. In fact, this concentration may be reached here at $\varepsilon = 0.15$, close to the strain where the maxima emerge.

Thus, the observed softening effect implicitly requires the occurrence of large concentrations of deformation-induced surplus vacancies, of the same order as thermally-induced ones at the melting temperature. One could object that it is impossible to differentiate between direct effects (strengthening effects by vacancies/clusters themselves) and indirect ones (vacancy-assisted climb of dislocations enabling dislocation rearrangement). However, it should be remarked that in most cases the direct effect implies a hardening, whereas vacancy/cluster annealing and rearrangements of dislocations always lead to softening. This is in agreement with the curves in Fig. 10; their shapes are not affected qualitatively by annealing

time, or, in other terms, any differences in shape of the fat and thin lines can be attributed solely to direct effects of vacancies/loops on the strength.

4.4. Alternative explanations of the effects observed

In the related literature, some objections have been raised that loop formation results from surface oxidation: O_2 atoms at the surface attract Zn atoms from the bulk which leave a growing number of vacancies here at increasing thickness of the surface layer thickness [16]. Although this process could doubtless be identified by X-ray topography in both bulk and foil samples [13, 14], it is improbable that it accounts for the actual results.

(i) The concentration of the loops shows a unique correlation with the amount of strain applied [19, 22]; the latter would have no detectable effect on loops caused by oxidation from the surface.

(ii) The "oxide" loops exhibit typical sizes of at least 3 μm, being a factor of 3–10 larger than those observed by our group (Figs 3a, b) and other authors [18–22] who have studied loops in deformed Zn crystals.

(iii) The growth rate of loops is at least a factor of 2 smaller than those observed in our investigations (Section 3.1.2 [9, 18, 19] and other comparable works [20, 21]; the whole growth process lasts up to a few months, largely exceeding the time intervals typical of actual anneal-hardening effects.

One could also consider some thermally activated processes of dislocation movement for the interpretation needed (pseudo-Peierls and cross-slip [38–40]). However, because of the constancy in temperature, none of these processes nor a combination of them can account for the complex isothermal behaviour observed (Figs 1, 2). Moreover, the increase in $\Delta\tau^*$ of the thermal stress component τ^* for fixed rate change $\Delta\dot{\varepsilon}$ remains unchanged before and after annealing treatment at $T_a = 293$ K [9]. This demonstrates that changes could occur in the athermal stress component only which strongly hints at some long-range interaction, e.g. the Orowan mechanism suggested in previous sections.

In the measurements in ZnAg, our interpretation by loop formation and/or coarsening may be criticized in view of other possible effects arising from local changes in concentration, single-phase transformations or precipitation of a second phase in the matrix. We sensibly restrict the discussion to these effects which do not resemble those of pure Zn; i.e. the strong increase of σ of heavily deformed Zn0.4Ag with annealing at $T_a = 293$ K. First, due to the coincidence of temperature of strength isotherms with that of deformation, neither a change in volume fraction of any second phase, nor a matrix concentration change, seem to be probable. Second, a rise of temperature (e.g. with annealing experiments as in [9]) should imply the dissolution of particles rather than the formation, resulting in a softening process in contrast to the drastic hardening observed instead.

4.5. Calculation of deformation-induced vacancy concentration, and comparison with experimental results

In principle, two types of model exist which yield the concentration of deformation-induced vacancies, c_v, as a function of strain, ε; these are

(I) the moving-jog (jog-dragging) models (e.g. by van Bueren [41, 42]), where the point defects arise from non-conservative movement of jogged screw dislocations

$$F \approx \varepsilon L N_f / \boldsymbol{b}^2 \tag{2}$$

(II) the more general ones like that of Saada [43, 44] which are based on the reaction of Hirsch [45] in considering the recombination of an edge dislocation dipole over a certain length

$$F = (A/G\boldsymbol{b}^3) \int \sigma \, d\varepsilon \tag{3}$$

where F is the number of vacancies per unit volume, L is the maximum distance between moving dislocations, N_f is the forest dislocation density, A a constant amounting to $A \approx 0.1$ [46], G the shear modulus, $\boldsymbol{b}$ the Burger's vector and σ is the actual stress applied.

Model I may appear somewhat unreal because the conservative movement of jogs is much more favourable from an energetic point of view. Nevertheless, when applying Models I and II in Stage I of deformation (see, for example, stress–strain curves in [9]), in both cases vacancy concentrations $c_v \approx 3 \times 10^{-7}$ result which fits well to measured values of forest dislocation density $N_f = 10^{-3}\,\text{cm}^{-2}$ [3–6] and dislocation mean free path $L = 0.2$ cm [1, 2]. They fit the TEM investigations less well (Fig. 3b, c, and [22]), from which c_v resulted to be 1–2 orders of magnitude larger: this, however, may again be caused by the strongly inhomogeneous distribution of vacancy loops in the deformed samples rather than by additional loop generation mechanisms as discussed in Section 4.4.

It should be emphasized here that the above value of c_v (although low) does suffice to yield a loop-induced hardening effect up to a factor of 2.5 even in Stage I, as has been observed in [9]: This c_v value and $d \approx 0.3$ μm (on average) yield $N_v \approx 1.34 \times 10^{10}\,\text{cm}^{-3}$. On inserting this into Equation 8 of Kirchner's paper [11] with the correct values of a and k, a strength increase by a factor of ~ 2.5 results. Thus, any suspicion that the forest dislocation density and, consequently, the loop density would be too small to account for the observed hardening, can be denied.

For the actual case of polycrystal deformation, Stage II versions of both models exist. Taking the most relevant part of Fig. 10a (solid line, $t_a = 15$ min) for a comparison with the resistivity experiment shown in Fig. 6c, the calculation according to Model II yields $c_v = 3.4 \times 10^{-5}$ (by choosing constant $A = 0.1$) which agrees very well with the c_v value from resistivity. However, the moving jog-model of van Bueren [41, 42] gives c_v values almost two orders of magnitude higher, and also cannot be applied in deformation stages higher than Stage II; considering Fig. 10, these ranges certainly are reached or even exceeded.

In conclusion, Saada's model is revealed as that most suitable to describe the actual polycrystal experiments; it also accounts satisfactorily for the experiments quoted above on single crystals [1, 2, 9].

5. Conclusions

1. Effects of anneal hardening on strength isotherms after intermediate-temperature/large-strain deformation are very similar to those after low-temperature/low-strain deformation, with regard to both shape and amount of the hardening observed.

2. Anomalies in isothermal annealing characteristics of strength can be related to an Orowan-type interaction of basal glide dislocations with prismatic vacancy loops, which undergo coarsening and/or depletion.

3. The measured amount of hardening/softening is in good correlation with the single vacancy concentrations obtained from resistivity measurements, and is also compatible with the loop diameters observed.

4. Saada's model is revealed to be the best in achieving the correct single vacancy concentrations.

5. Oxidation-induced loop formation can be ruled out, because of significant differences in size and growth kinetics compared with deformation-induced loops; phase transformations are shown to cause softening in all cases, and thus they cannot account for the hardening effects repeatedly observed.

6. Deformation-induced surplus vacancies not only affect the stress–strain relationship by loop formation, but also help dislocations to climb and may induce a general dislocation rearrangement, which leads to marked softening effects in ranges of large strain.

Acknowledgements

The authors thank Professor F. Stangler for his general support of this work, Professor G. Schöck for many fruitful discussions and constructive remarks to the manuscript, and Dr B. Mikulowski for the provision of two transmission electron micrographs and fruitful comments.

References

1. A. SEEGER and H. TRÄUBLE, *Z. Metallkde* **51** (1960) 435.
2. A. SEEGER, H. KRONMÜLLER, S. MADER and H. TRÄUBLE, *Phil. Mag.* **6** (1961) 639.
3. K. H. ADAMS, T. VREELAND Jr and D. S. WOOD, *Mater. Sci. Engng* **2** (1967) 37.
4. F. F. LAVRENTEV, O. P. SALITA, P. D. SHUTYAYEV, *Phys. Met. Metall.* **41** (1976) 412.
5. F. F. LAVRENTEV and V. L. VLADIMIROVA, *Mater. Sci. Engng* **30** (1977) 141.
6. F. F. LAVRENTEV, O. P. SALITA and P. D. SHUTYAYEV, *Phys. Met. Metall.* **43** (1977) 1300.
7. M. BOCEK, *Phys. Status Solidi* **3** (1963) 2169.
8. B. WIELKE, *Phys. Status Solidi (a)* **33** (1976) 241.
9. B. MIKULOWSKI, B. WIELKE and H. O. K. KIRCHNER, *Acta Metall.* **30** (1982) 633.
10. B. WIELKE, A. CHALUPKA and G. SCHÖCK, in "Proceedings ICSMA 5", Aachen, edited by P. Haasen *et al.* (Pergamon Press, Oxford, 1979) p. 65.
11. H. O. K. KIRCHNER, *Z. Metallkde* **67** (1976) 525.
12. J. SPYRIDELIS, *Mater. Res. Bull.* **6** (1971) 1345.
13. S. J. BURNS and B. RÖSSLER, *Phys. Status Solidi (a)* **13** (1972) K91.
14. D. MICHELL and G. J. OGILVIE, *Phys. Status Solidi* **15** (1968) 83.
15. C. G'SELL, PhD thesis, Inst. Nat. Polytechn. de Lorraine, Nancy, France (1977).
16. R. E. SMALLMAN and K. H. WESTMACOTT, *Mater. Sci. Engng* **9** (1972) 249.
17. M. ZEHETBAUER and D. TRATTNER, *ibid.* **89** (1987) 93.
18. B. MIKULOWSKI and B. WIELKE, *Czech. J. Phys. B* **35** (1985) 286.
19. *Idem, ibid.* **38** (1988) 453.
20. A. BERGHEZAN, A. FOURDEUX and S. AMELINCKX, *Acta Metall.* **9** (1961) 464.
21. H. MÜLLER, Thesis, Technische Universität Braunschweig, FRG (1983).
22. W. PFEIFFER, *Phys. Status Solidi* **2** (1962) 1727.
23. R. W. CAHN, in "Physical Metallurgy", edited by R. W. Cahn and P. Haasen (Elsevier, Amsterdam, 1983) Ch. 25, p. 1595.
24 J. NIHOUL, *Phys. Status Solidi* **3** (1963) 2061.
25. P. EHRHARDT and B. SCHÖNFELD, *Phys. Rev. B* **19** (1979) 3896.
26. *Idem, ibid.* **19** (1979) 3905.
27. C. HIDALGO, S. LINDEROTH and N. de DIEGO, *Phil. Mag.* **A54** (1986) L 61.
28. C. HIDALGO, N. de DIEGO and P. MOSER, *J. Appl. Phys.* **A40** (1986) 25.
29. M. ZEHETBAUER, J. SCHMIDT and F. HAESSNER, *Scripta Metall.* **25** (1991) 559.
30. H. J. WOLLENBERGER, in "Physical Metallurgy", edited by R. W. Cahn and P. Haasen (Elsevier, Amsterdam, 1983) Ch. 17, p. 1139.
31. J. SCHMIDT, unpublished results, Technische Universität Braunschweig, FRG (1989).
32. H. KIMURA and R. MADDIN, in "Quench Hardening in Metals" (North Holland, 1971) p. 30.
33. D. M. FEGREDO, *J. Inst. Metals* **93** (1964/65) 268.
34. M. ZEHETBAUER, *J. Phys. Cond. Matt.* **1** (1989) 2833.
35. S. CERESARA, H. ELKHOLY and T. FEDERIGHI, *Phil. Mag.* **12** (1965) 1105.
36. F. HAESSNER and J. SCHMIDT, *Scripta Metall.* **22** (1988) 1917.
37. M. DEIGHTON and R. N. PARKINS, *Trans. Met. Soc. AIME* **245** (1969) 1917.
38. A. COURET and D. CAILLARD, *Acta Metall.* **33** (1985) 1447.
39. *Idem, ibid.* **33** (1985) 1455.
40. G. SCHÖCK and W. PÜSCHL, in "Proceedings of the 8th International Conference on Strength of Metals and Alloys", (ICSMA 8), Tampere, Finland, edited by P. O. Kettunen, T. K. Lepistö and M. E. Lehtonen (Pergamon Press, Oxford, 1988) p. 239.
41. H. G. van BUEREN, *Acta Metall.* **3** (1955) 519.
42. *Idem*, in "Imperfections in Crystals" (North Holland, 1960) p. 153.
43. G. SAADA, *Acta Metall.* **9** (1961) 166.
44. *Idem, ibid.* **9** (1961) 965.
45. P. B. HIRSCH, in "Internal Stresses and Fatigue in Metals", edited by G. M. Rasweiler and W. L. Grube (Elsevier, 1959) p. 139.
46. A. v. d. BEUKEL, in "Vacancies and Interstitials of Metals", edited by A. Seeger, D. Schumacher, W. Schilling and J. Diehl (North Holland, Amsterdam, 1969) p. 427.

Received 26 July
and accepted 30 November 1990